

Electron-impact detachment from negative ions

L. Vejby-Christensen, D. Kella, D. Mathur,* H. B. Pedersen, H. T. Schmidt, and L. H. Andersen
Institute of Physics and Astronomy, University of Aarhus, DK 8000, Aarhus C, Denmark

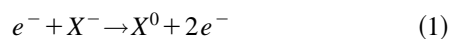
(Received 3 October 1995)

Electron-impact detachment cross sections have been measured from threshold to about 30 eV for D^- and O^- . The purpose was to investigate the cross section near threshold and to reinvestigate earlier claims of resonances due to short-lived states of the doubly charged negative ion. Initial results for D^- showed no resonances [L. H. Andersen, D. Mathur, H. T. Schmidt, and L. Vejby-Christensen, *Phys. Rev. Lett.* **74**, 892 (1995)]. Here we show that there is no detectable resonance structure for O^- either. The applied experimental technique is discussed in detail. Classical and semiclassical models for the detachment process are presented and compared with the data.

PACS number(s): 34.80.-i, 41.75.Cn, 71.27.+a, 34.50.-s

I. INTRODUCTION

Electron-impact ionization of atoms and ions has been studied since the early days of quantum mechanics, and much of our understanding of the structure of atoms emerged from scattering experiments with electrons [1–3]. In this work, we address the problem of electron-impact detachment from negative ions. The first experiments of this kind were conducted by Tisone and Branscomb [4,5] and by Dance, Harrison, and Rundel [6]. Both groups measured the detachment cross section of H^- from around 10 to 500 eV, and Tisone and Branscomb also did an investigation on O^- . Later, Peart, Walton, and Dolder studied H^- [7] and other systems such as C^- , O^- [8], and F^- [9]. Cross sections for electron-impact detachment are large. The experimental groups generally agreed that, for H^- , the cross section is between $\sim 3 \times 10^{-15}$ and $\sim 5 \times 10^{-15}$ cm² at the cross-section maximum at about 10–20 eV. Here we consider the detachment reaction between an electron and a negative ion X^- ,



($X = D$ or O), from threshold and up to about 30 eV. None of the earlier experiments were carried out at sufficiently low energy that the threshold region could be studied.

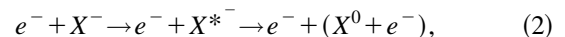
As to theory, several groups have performed Born-type calculations on H^- [10–14], but the results differ very significantly, in particular in the region around the maximum. According to Bely and Schwartz [13], the requirement of orthogonality of the initial and final wave functions is crucial, and the value of the cross-section maximum appeared to decrease with increasing accuracy of the calculations. The lowest maximum value of $\sim 3 \times 10^{-15}$ cm² was obtained by Bely and Schwartz [13].

As already mentioned, we shall be particularly interested in the threshold region. For electrons incident on positive ions or neutral atoms and for incident photons on negative ions, ionization and detachment are well described here by

the Wannier theory [15] and by the Wigner law, respectively [16,17]. With electrons impinging on negative ions, the situation turns out to be somewhat different. There is a strong Coulomb repulsion in the incoming channel, and the collision is adiabatic. The detachment process has been described by tunneling through a barrier [11,18], and we shall compare our measured cross sections to predictions of this picture and to results of a simple classical model. For the threshold limit, Hart, Gray, and Guier [19] calculated a cross section which increases exponentially with energy. If such a dependence exists, it must be within the region where we find no detectable cross section.

Negative ions differ in many respects from neutral atoms. First, the binding energy is much smaller in negative ions. Second, the charge of the ion results in a Coulomb repulsion in the incoming channel that is absent for atoms, where only polarization forces are present at large distances. Third, the negative ions do not have an infinite series of excited states but only a few, if any. The presence of excited autoionizing states is important for atoms and positive ions since it may lead to structures in the ionization cross section. Structures in the electron-impact ionization cross section of neutral Hg was discovered as early as 1926 by Lawrence [20]. It remains to be seen if autodetaching states of negative ions yield similar structures in the electron-impact detachment cross section.

There are in principle two different categories of processes which involve resonances. In one of them, the negative ion is first excited to a resonant state that lies in the continuum and, subsequently, this state autodetaches:

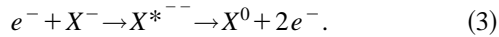


where the asterisk indicates an excited ion. The result of the combined reaction is detachment from the negative ion. Note that the resonant character of the process is relaxed since the first step of the reaction may happen at any incident electron energy above the excitation energy. The process for atoms and positive ions is known as excitation autoionization (EA), and with negative ions one may call the process excitation autodetachment (also EA). It was first observed in the ionization of Ba^+ [21], and manifested itself as an abrupt increase in the cross section at the opening of the excitation

*Permanent address: Tata Institute of Fundamental Research, Bombay 400 005, India.

channel. For positive ions with complex electronic structure, the EA process may dominate over direct outer-shell ionization by an order of magnitude (see, e.g., [3,22]).

In the other process, the incoming electron is captured into a resonance state of the doubly charged negative ion that subsequently decays by the emission of two electrons:



This is a true resonant process in the sense that the incoming electron energy has to match the resonance energy. One may call this process resonant-excitation double autodetachment (REDA), in analogy to resonant-excitation double autoionization [23]. It is similar to the dielectronic-capture process that leads to dielectronic recombination with positive ions. However, the resonance width may be substantial due to the short lifetime of the resonance state of the doubly charged negative ion. Thus it is not clear at the onset whether resonances will be perceivable in the electron-impact detachment cross section at all. On the other hand, if resonances due to the reaction in Eq. (3) are observed, they provide evidence for the existence of doubly charged negative atomic ion states (X^{*-}).

Walton, Peart, and Dolder reported on the observation of two resonances in the electron-impact detachment cross section of H^- [24–26]. The resonances were observed at incident electron energies of about 14.5 and 17.2 eV, and were attributed to short-lived H^{--} states, and thus of the REDA type [Eq. (3)]. The measured widths of the observed structures implied lifetimes of the order of 10^{-15} s. The resonances were soon after their discovery classified as $2s^2 2p(2P^o)$ and $2p^3(2P^o)$ by Taylor and Thomas [27,28]. Later, structures in the cross section for O^- were reported [29], whereas no structures were noticed for C^- . With the experimental observation and the theoretical interpretation, the subject of resonances in electron-negative ion scattering seemed understood, in particular for H^- . Nevertheless, in a recent comprehensive theoretical paper [30], it was argued that the size of the observed resonances would violate unitarity of the collision matrix, and direct calculations showed no evidence for resonances associated with H^{--} . Furthermore, resonances were not expected at an energy above the total breakup energy of the Coulomb system. At the same time, the scattering experiment was repeated, this time on D^- , and no sign of the resonances was found [31]. In the present work we have continued the search for structures that may be related to the EA and REDA types of resonances.

Dinegative ions with long ($> 10^{-5}$ s) lifetimes have been reported by groups using mass spectrometers. However, many of the results have later been questioned by other researchers [32]. For references to the subject, one may consult the paper by Christophorou [33].

Experimentally, it is difficult to produce intense electron beams with an energy that matches the low binding energy of negative ions, and hence the crossed-beams technique is not well suited for threshold studies of electron-impact detachment. In the merged-beams configuration, on the other hand, with fast ion beams, one can study the low-energy threshold region with electron beams of \sim keV energy. This is a tremendous advantage since higher electron densities and better energy resolution may then be obtained. The latter is due to

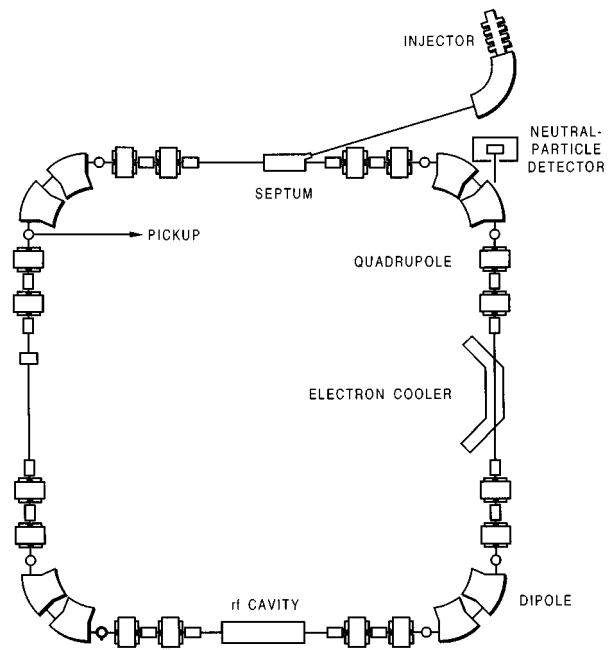


FIG. 1. The ASTRID storage ring with the electron cooler.

the kinematic compression. Further, high-energy ion beams are associated with smaller cross sections for neutralization in the residual gas. The merged-beams technique has been applied successfully in low-energy electron-ion recombination studies (see, e.g., [34,35]).

In heavy-ion storage rings, electron coolers provide the electrons for the merged-beams experiments. Electron coolers are devices where intense electron beams (typical density of the order of 10^7 cm $^{-3}$) are merged with fast ion beams (\sim MeV/amu) in order to “momentum cool” the circulating ions [36]. In studies of electron-impact phenomena and in particular threshold behavior and resonances, it is crucial that the electron-velocity distribution in the experiment is known. The properties of electron coolers, where the electron beam is guided by a longitudinal magnetic field of typically several hundred G, have been discussed in several papers (see, e.g., [36–38]). The characteristic properties (temperatures) of the velocity distribution may be obtained directly by measurements of narrow dielectronic-recombination resonances [37], through comparisons of the measured electron-cooling forces in storage rings with theory [39], and may also be estimated from the measured rate of neutral-atom formation due to radiative recombination behind the cooler [36].

II. EXPERIMENT

The present experiment was conducted at the Aarhus Storage Ring Denmark (ASTRID). The ring has a perimeter of 40 m and two bending magnets in each of the four corners (see Fig. 1). The negative ions were directed into ASTRID from an injector that was operated at 150 kV. A duoplasmatron ion source was used to produce a ~ 5 - μ A D^- beam. The O^- beam was conveniently produced by a sputter-ion source. After injection into the ring, the ions were accelerated by a rf cavity. The maximum magnetic rigidity of ASTRID is 1.93 T m. This yields a maximum storage energy given by

$$E_{\max} = 931.5(\sqrt{0.3744q^2 + M_i^2} - M_i) \text{ MeV}, \quad (4)$$

where q is the ion charge in units of e , the elementary charge, and M_i is the mass of the stored ion in amu. Acceleration is normally accomplished within a few seconds. After acceleration to several MeV, the beam-storage lifetime for negative ions is about 1–5 s at the average ring pressure of $\sim 3 \times 10^{-11}$ mbar. The corresponding lifetime for positive molecular ions is typically 10–30 s, whereas protons may survive for many hours.

The electrons were delivered by an electron cooler (see Fig. 1) which can produce electron beams of about 1–100 mA with energies between ~ 50 and 2000 eV [37]. At a given kinetic energy E_e of the electrons in the laboratory frame, the relative electron energy E is determined from

$$E = \frac{1}{2}m(v_i - v_e)^2 = \left[\left(\frac{m}{M_i} \right)^{1/2} - \sqrt{E_e} \right]^2, \quad (5)$$

where m is the electron mass, v_i and v_e are the laboratory velocities of the ions and electrons, respectively, and E_i is the ion-beam energy. The laboratory energy E_e was found from the relation

$$E_e = -eV_c + eV_s, \quad (6)$$

where V_c is the cathode potential and V_s is the space-charge potential which was typically a few V. V_s was found by adjusting V_c until $v_e = v_i$ (the cooling condition), as observed on the ion-Schottky signal. Knowing V_c , E_i , and the fact that $E=0$ at cooling, Eqs. (5) and (6) yield V_s . The space-charge potential may also be calculated directly from the known beam geometry and the electron current. We found good agreement between the calculated value and that determined from the observed cooling condition, implying little ion and electron trapping in the interaction region.

The electron-beam profile has been measured earlier [37]. The electron-beam density is essentially uniform and is given by

$$\rho_e = \frac{I_e}{\pi r^2 v_e e}, \quad (7)$$

where r is the electron-beam radius, which could be adjusted to be between 0.5 and 2.2 cm (see later discussion), and I_e is the electron-beam current.

The detachment reaction [Eq. (1)] was identified by detecting the neutral atoms behind the bending magnet after the interaction with the electrons in the electron cooler. For this purpose, a 25-mm-diameter channel-plate detector was used. Since the ion-beam diameter is smaller than the electron-beam diameter, and the electron density is constant to a good approximation [36], the rate of detected neutrals $N(X^0)$ is given by

$$N(X^0) = \varepsilon \frac{N(X^-)}{v_i} l \rho_e v \sigma + N_0(X^0), \quad (8)$$

where σ is the detachment cross section, v the relative velocity $(2E/m)^{1/2}$, ε the detection efficiency, l ($=85$ cm) the effective length of the interaction section, $N(X^-)$ the number of ions entering the interaction region per unit time, and

$N_0(X^0)$ the background contribution due to detachment in the residual gas and in the toroid regions (see later discussion). Typically, $[N(X^0) - N_0(X^0)]/N_0(X^0)$ was about 1, which is about 50–100 times more than in the early experiments [4–6]. Moreover, with the present technique, there are no slit-scattered particles that may rise to false signals in the ion detector and hence cause an overestimate of the cross section.

Due to the finite electron-velocity spread in the rest frame of the ion beam, we extract from the measured quantities the “rate coefficient” given as

$$\langle v \sigma \rangle = \frac{N(X^0) - N_0(X^0)}{N(X^-)} \frac{v_i}{l \varepsilon \rho_e}, \quad (9)$$

which may be compared with a calculated rate coefficient when the cross section $\sigma(v)$ is known:

$$\langle v \sigma \rangle = \int v \sigma(v) f(v) dv. \quad (10)$$

The electron-velocity distribution function $f(v)$ is described as

$$f(v) = \left(\frac{m}{2\pi k T_{\perp}} \right) e^{-mv_{\perp}^2/2kT_{\perp}} \left(\frac{m}{2\pi k T_{\parallel}} \right)^{1/2} e^{-m(v_{\parallel} - \Delta)^2/2kT_{\parallel}}, \quad (11)$$

where v_{\perp} and v_{\parallel} are the electron-velocity components perpendicular and parallel to the ion-beam direction, respectively, and Δ is the detuning velocity.

Without adiabatic expansion of the electron beam ($r=0.5$ cm), the beam temperatures were $kT_{\perp}=0.1-0.15$ eV and $kT_{\parallel}=10^{-4}-10^{-3}$ eV [37]. To improve the transverse temperature, the electron beam could be adiabatically expanded by a factor of up to 20 by means of a magnetic field of up to 2 kG in the electron-gun region, and a 100-G field in the interaction region. The electron beam expands as the magnetic field decreases, and the transverse temperature changes proportionally to the field. Thus the adiabatic expansion results in a larger electron-beam diameter, and the transverse temperature can be reduced to below 0.01 eV [40]. To illustrate the resolution in the experiment, we show in Fig. 2 the calculated rate coefficient $\langle v \sigma \rangle$ [Eq. (10)] for an infinitely sharp resonance located at $E=8$ eV, which is a typical relative electron energy in the experiment to be reported. For a vanishing transverse velocity spread, the longitudinal temperature leads to a full width $2(EkT_{\parallel})^{1/2}$, equal to 0.13 eV in the example shown in Fig. 2. Transverse temperatures below this value have only a moderate influence on the resonance.

Relative rate coefficients are easily obtained when we assume that $N_0(X^0)$ is proportional to $N(X^-)$. Absolute rate coefficients may be obtained directly from Eq. (9) when the detector efficiency ε and $N(X^-)$ are known. The detector efficiency could be measured for any detector type by comparing count rates with that of a solid-state detector, the efficiency of which is unity at MeV particle energies. $N(X^-)$ was in the measurement with O^- known from a current-transformer device. However, in our early measurements with D^- , this device was not available, and the absolute rate

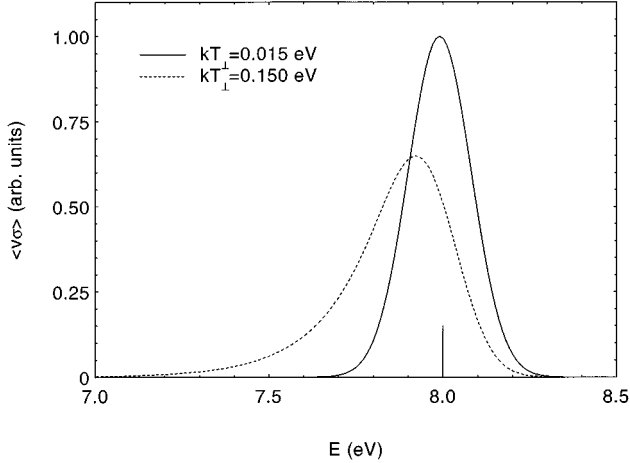


FIG. 2. The rate coefficient $\langle v\sigma \rangle$ calculated for an infinitely narrow resonance at $E=8$ eV. The full curve is calculated for a factor of 10 adiabatic expansion ($kT_{\perp}=0.015$ eV and $kT_{\parallel}=5 \times 10^{-4}$ eV). The dashed curve corresponds to an unexpanded electron beam ($kT_{\perp}=0.15$ eV and $kT_{\parallel}=5 \times 10^{-4}$ eV). The FWHM's for the peaks are 0.22 and 0.30 eV.

coefficient was deduced from the change in the beam-storage lifetimes due to detachment by the electrons. The rate coefficient may be expressed as

$$\langle v\sigma \rangle = (k - k_0) \frac{L}{l} \frac{1}{\rho_e}, \quad (12)$$

where L is the perimeter of the ring, k is the total decay rate, and k_0 is the background decay rate primarily due to collisions with the residual gas. k_0 was measured at $E=0$. The decay rate was found from a fit of the count rate of neutrals as a function of time to an exponential function $\exp(-kt)$. Measurements were performed at a fixed ion energy and varying electron energy. In Fig. 3 is shown the variation of the decay rate with electron energy for 4-MeV D^- . The absolute normalization for D^- is estimated to be accurate to within $\pm 40\%$. The accuracy for O^- is $\pm 20\%$ since a more

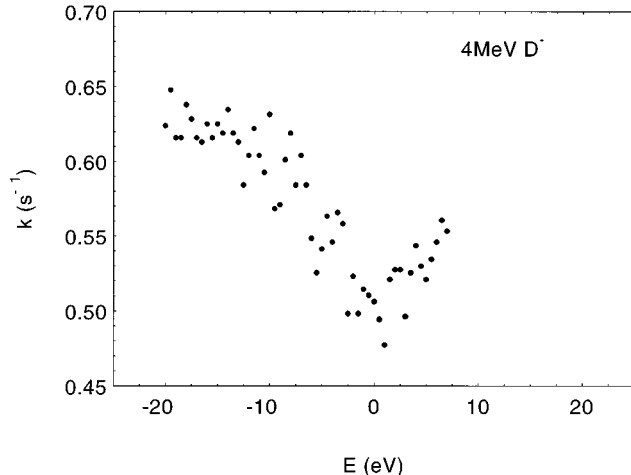


FIG. 3. The decay constant k as a function of energy measured for 4-MeV D^- (negative energies have $v_e < v_i$ and positive energies have $v_e > v_i$).

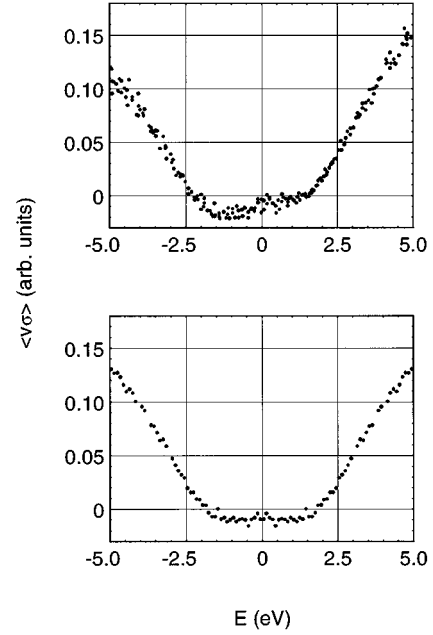


FIG. 4. The rate coefficient $\langle v\sigma \rangle$ for detachment from D^- near threshold obtained from Eq. (9). $N_0(X^0)$ was assumed to be proportional to $N(X^-)$. Upper graph: the result when $N(X^0) - N_0(X^0)$ was determined by the modulation technique (see text). Lower graph: the symmetrized data (averaged over data for $v_e > v_i$ and $v_e < v_i$).

accurate current transformer was used in this case. The scattering within a measurement is typical for the relative uncertainty.

To determine $N(X^0)$ and $N_0(X^0)$, the electron beam could be turned on and off (chopped) at a frequency higher than the inverse vacuum response time (~ 10 Hz). This ensured that the pressure during the measurement of $N(X^0)$ (when electrons were on) was the same as when the electrons were turned off for measurement of $N_0(X^0)$. At $E=0$ (the cooling condition where $v_i = v_e$), a small difference between $N(X^0)$ and $N_0(X^0)$ measured in this way was observed. This could not be ascribed to detachment by the electrons in the merge region since here $E < E_B$, where E_B is the electronic-binding energy of the negative ion. However, in the toroid regions, where the two beams gradually merge and separate, the relative energy is sufficient to detach electrons. To minimize this effect, the electron cooler was operated in another mode, where the energy was changed (modulated) between the relative energy E and $E=0$, again faster than the vacuum response time. When $E=0$, the measured yield $N_0(X^0)$ had contributions from the merge and demerge regions as well as from interactions with the residual gas in the ring. Clearly, $N(X^0) - N_0(X^0)$, and hence $\langle v\sigma \rangle$, is almost zero at $E=0$, as expected since the two quantities $N(X^0)$ and $N_0(X^0)$ are measured under equal conditions; see Fig. 4. There is, however, a small difference between $N(X^0)$ and $N_0(X^0)$ in the region $0 < E < E_B$, which is due to the fact that, in this energy region, the toroid-region contribution is slightly different from that at $E=0$. To minimize this effect, we present our data as the average of the contributions from $E < 0$ ($v_e < v_i$) and $E > 0$ ($v_e > v_i$). This averaging procedure results in a cross section which is essentially constant below ~ 2 eV.

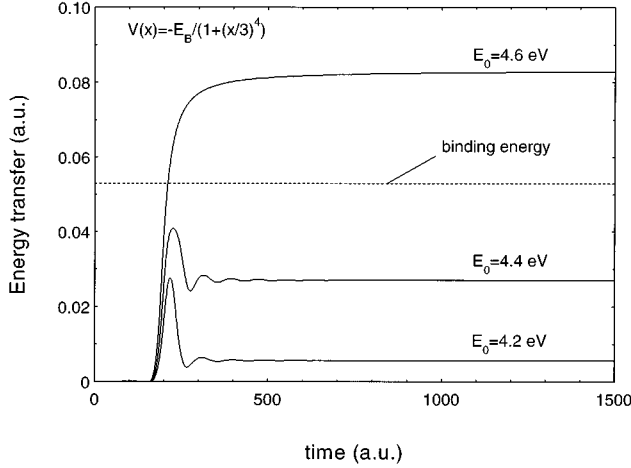


FIG. 5. The one-dimensional dynamic simulation. Shown is the energy transfer as a function of time for O^- for four different incident energies.

This constant defined the level for zero cross section. The D^- data were taken at two different storage energies and resulted in essentially identical cross sections, as shown below.

III. RESULTS AND DISCUSSION

A. Detachment cross sections

We have described the detachment process classically in the energy region around the threshold. To make the problem simple to handle, we first consider only zero impact-parameter collisions. This should not be a bad approximation close to the threshold. The problem is easily handled in a one-dimensional model. The active target electron is assumed to be bound in the usual short-range potential ($1/r^4$). In the model, we choose a simple binding potential with the correct asymptotic behavior of the form (we use atomic units unless otherwise specified)

$$V_B(x) = \frac{-E_B}{1 + (x/a)^4}, \quad (13)$$

where a is a measure of the size of the ion ($\sim 4-5$ for H^- and D^- , and ~ 3 for O^-) [41], and E_B is the binding energy or electron affinity of the negative ion (2.76×10^{-2} for H^- and D^- , and 5.37×10^{-2} for O^-). We performed a dynamic simulation of the scattering process with one bound electron, initially at rest, in the potential $V_B(x)$. In Fig. 5 is shown the energy transfer as a function of time for O^- at three different incident energies. It is seen that the energy transfer exceeds the binding energy for incident energies between 4.4 and 4.6 eV, which is ~ 3 times the binding energy. The adiabatic nature of the collision process is also seen in the figure. Below threshold (at ~ 4.5 eV), the target electron is able to absorb energy and then transfer a substantial part of it back to the incoming electron. As observed in Fig. 6, the perturbing force on the target electron must exceed the maximum binding force of the potential $V_B(x)$ to result in detachment. The binding force is $-\partial V/\partial x$ and the maximum perturbing force is approximately $1/D_0^2 = E^2$, where D_0 is the distance of closest approach and E is the initial electron energy. By

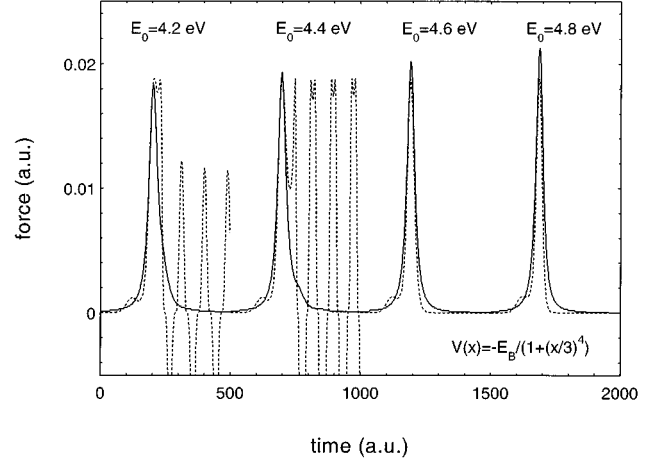


FIG. 6. The one-dimensional dynamic simulation. Shown are the binding force (dashed curve) and the perturbing force (full curve) as a function of time for O^- for four different incident energies. Each energy is shown for a time span of 500 a.u.

balancing the binding and perturbing forces, the detachment-threshold energy may for the present model potential be expressed as

$$E_{th} \approx \sqrt{E_B/a}. \quad (14)$$

The value of the threshold energy obtained from Eq. (14) is slightly lower than that found from the dynamic simulation. This is due to the fact that in the dynamic simulation, the electron is pressed away from the incoming electron, while in the derivation of Eq. (14) the perturbing force is calculated assuming the target electron is at the origin.

On the assumption that the incoming electron experiences a purely repulsive Coulomb potential, the distance of closest approach as a function of the impact parameter ρ is given by

$$D(\rho) = \frac{1}{2}D_0 + \sqrt{\left(\frac{1}{2}D_0\right)^2 + \rho^2}. \quad (15)$$

If it is assumed that detachment takes place with a constant probability p when the incoming electron gets inside a reaction radius R , the cross section may be expressed as

$$\begin{aligned} \sigma &= 2\pi \int_0^\infty \rho \, d\rho \begin{cases} p; & D(\rho) \leq R \\ 0; & D(\rho) > R \end{cases} \\ &= p\pi R^2 \max \left[0, \left(1 - \frac{E_{th}}{E} \right) \right], \end{aligned} \quad (16)$$

where we have introduced the threshold energy as $E_{th} = 1/R$.

As seen in Figs. 7 and 8, this classical reaction model reproduces the general behavior of our experimental data remarkably well when the reaction radius R is about 15 for D^- and 8 for O^- . Note that p is just a scaling factor which has no influence on the shape of the cross section. We obtain a value $p \sim 10-20\%$ which is considerably less than 1. There

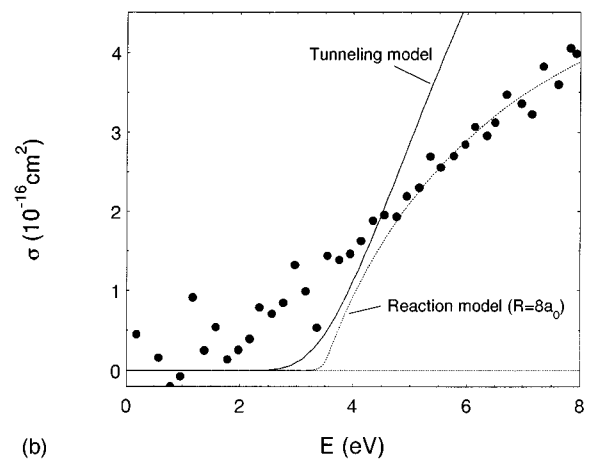
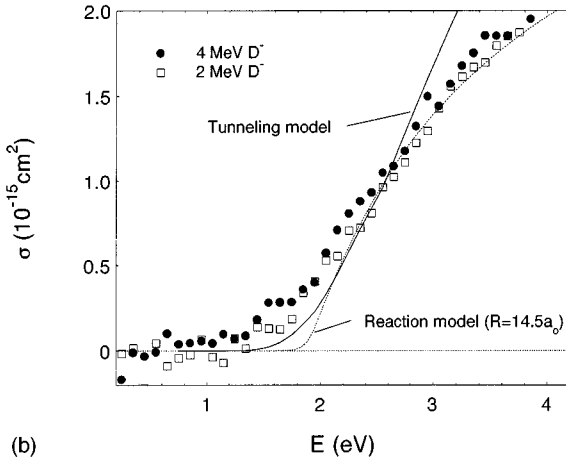
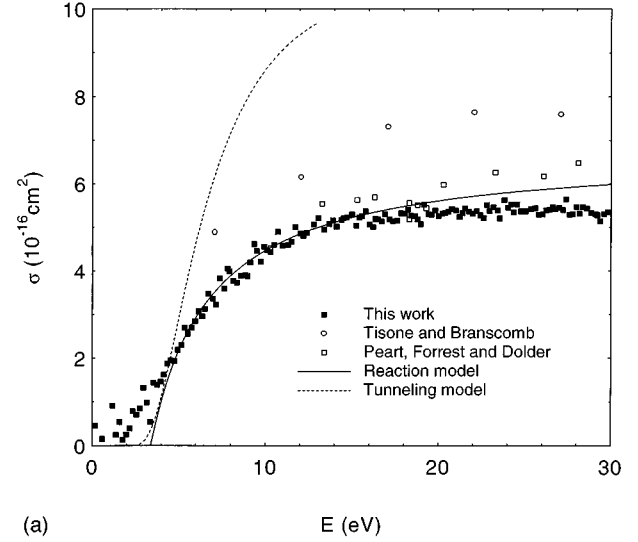
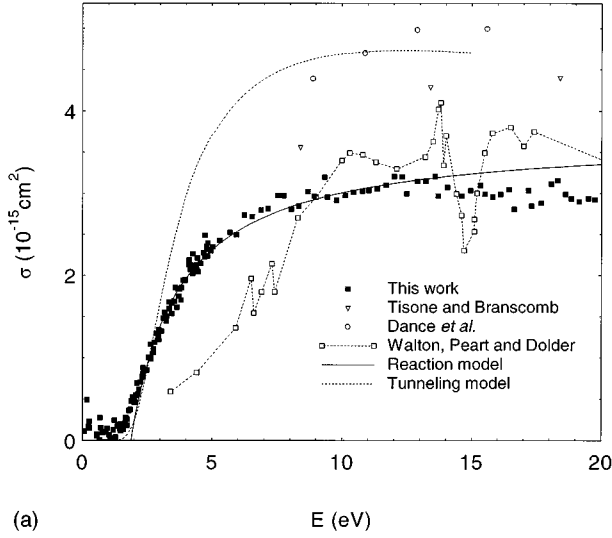


FIG. 7. (a) The average cross section $\langle v\sigma \rangle/v$ as a function of energy for D^- . Shown are the results of the classical reaction model and the tunneling model. The cross sections have been folded with the velocity distribution of Eq. (11) with $kT_{\perp} = 0.030$ eV and $kT_{\parallel} = 5 \times 10^{-4}$ eV (adiabatic expansion with a factor of 5). Earlier experimental results [5,6,25] are shown for comparison. (b) Like (a) in the threshold region.

FIG. 8. (a) The averaged cross section $\langle v\sigma \rangle/v$ as a function of energy for O^- . Shown are the results of the classical reaction model and the tunneling model. The cross sections have been folded with the velocity distribution of Eq. (11) with $kT_{\perp} = 0.030$ eV and $kT_{\parallel} = 5 \times 10^{-4}$ eV (adiabatic expansion with a factor of 5). Earlier experimental results [5,8] are shown for comparison. (b) Like (a) in the threshold region.

is some uncertainty about the absolute scale of our experimental data, as discussed in Sec. II. However, even with the largest absolute cross sections obtained by other experimental groups [4–6], the value of p is less than one-half. The results of the classical reaction model together with values fitted to the data are summarized in Table I. Note that the model predicts threshold energies [Eq. (14)] that are much higher than the binding energies. Classically, this is understandable since it requires energy to get close enough to release the bound electron, and, after release, the two continuum electrons carry away excess energy due to the mutual repulsion.

To apply classical mechanics, large angular-momentum values are required, $L = vr \gg 1$. With $r \sim (\sigma/\pi)^{1/2}$ and $\sigma \sim 10^{-15}$ cm², we find that the energy of the projectile electron must be larger than about 1 eV. Thus there is some hope that a classical description is valid well above threshold. Close to threshold, the applicability of the classical model is probably more doubtful.

We have also considered the problem in a semiclassical way. The electric field of the incoming electron perturbs the binding potential, and escape becomes possible via *tunneling*. This is in particular important in the low-energy region. At higher energies, the perturbing field becomes sufficiently strong that escape can take place without tunneling. The situation is illustrated in Fig. 9 for the one-dimensional model. The perturbing force provides a potential which, in the limit of a constant field, becomes $V_p(x) = -E^2x$ when the force is

TABLE I. Comparison between the classical reaction model [Eq. (14)] and experimental fit [Eq. (16)]. a_0 is the Bohr radius.

Ion	E_B (eV)	$R(\text{fit})$	$E_{\text{th}} = 1/R(\text{fit})$ (eV)	$p(\text{fit})$	$a(\text{model})$	$E_{\text{th}}(\text{model})$ (eV)
D^-	0.75	$14.5a_0$	1.9	0.20	$5a_0$	2.0
O^-	1.46	$8a_0$	3.4	0.12	$3a_0$	3.6

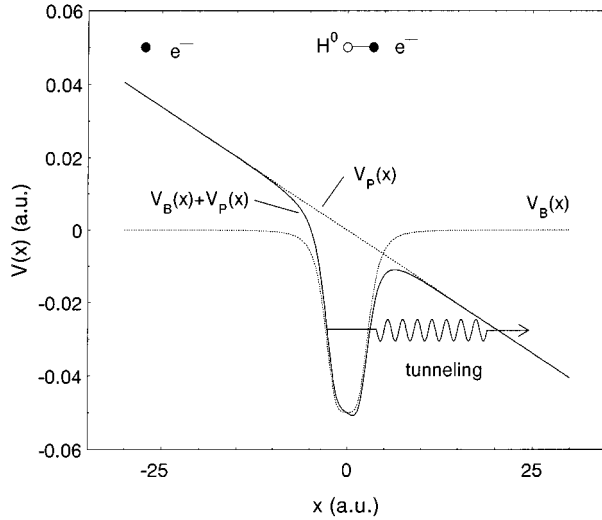


FIG. 9. The one-dimensional model for detachment of H^- illustrated for a kinetic energy $E=1$ eV. Shown are the perturbing and binding potentials (in a.u.), as discussed in the text.

taken at its maximum value. This creates a barrier through which the electron must tunnel to escape.

The problem of electron-impact detachment via tunneling was treated by Smirnov and Chibisov [11] and by Demkov and Drukarev [18]. The theory has been applied to calculate the cross section for H^- neutralization by impact of antiprotons or H^- [42]. It is assumed that the negative ion is associated with a three-dimensional well with negligible extension. This is a good approximation when the field from the projectile electron is weak. The tunneling-decay probability per unit time W in the limit of a *constant* electric field F was calculated as

$$W = \frac{A^2 F}{\sqrt{8E_B}} \exp \left[- \left(\frac{32 E_B^3}{9 F^2} \right)^{1/3} \right], \quad (17)$$

where A^2 is 2.65 for D^- [11] and 1.35 for O^- [41]. For a *Coulomb* field, the following expression for W was found:

$$W = \frac{A^2 F}{\sqrt{8E_B}} \exp \left[- \left(\frac{8E_B}{F} \right)^{1/2} f \left(\frac{E_B}{\sqrt{F}} \right) \right], \quad (18)$$

$$f(x) = \frac{\arcsin \sqrt{x}}{\sqrt{x(1-x)}} - 1.$$

The Coulomb field at the negative ion is $F = [1/R_D(\rho, t)]^2$, where $R_D(\rho, t)$ is the radial distance between the incoming electron and the negative ion as a function of time and impact parameter.

The decay probability as a function of impact parameter may be expressed as

$$P(\rho) = 1 - \exp \left(- \int_{-\infty}^{+\infty} W(R_D(\rho, t)) dt \right), \quad (19)$$

and the cross section is

$$\sigma = 2\pi \int_0^{\infty} P(\rho) \rho d\rho, \quad (20)$$

which is calculated numerically. The results are shown in Figs. 7 and 8, where experimental data from previous works are also shown. The decay probability as a function of impact parameter $P(\rho)$ turns out to be significantly less than one for many impact parameters smaller than the classical reaction radius. This explains why the probability p in the classical model turns out to be smaller than 1.

The energy range in which the model is applicable is limited. An upper limit is set by the requirement that the incoming electron does not change the binding energy of the negative ion significantly. A rough estimate based on the polarizability of the negative ion yields $E < 3.4$ eV for D^- . The model accounts reasonably well for the onset of the cross section near threshold; however, the shape in the threshold region is not perfect. The value of A^2 used for O^- is somewhat uncertain, as discussed by Esaulov [43], and the absolute value found in the model may thus be in error. As a curiosity, we may mention that if one uses the constant-field limit for W [Eq. (17)], the model yields a cross-section behavior with a perfect shape, but an absolute value which is a factor of ~ 2 higher than our measured data.

B. Resonance structure

Since O^{--} has a Ne-like closed-shell structure, it might be expected that this system in particular should have a lifetime sufficiently long to provide detectable structures in the electron-impact detachment cross section. Herrick and Stillinger [44] performed variational calculations and predicted an O^{--} resonance at 5.38 eV with a width of 1.3 eV. Gadzuk and Clark [45] calculated a resonance energy of 8.8 eV, and Huzinaga and Hart-Davis [46] obtained 7.68 eV. The latter is close to the value of 7.2 eV predicted from an extrapolation of the $1s^2 2s^2 2p^6$ (1S_0)-state energy of the isoelectronic sequence for Si^{4+} , Al^{3+} , Mg^{2+} , Na^+ , Ne , and F^- [30].

In the experimental work by Peart, Forrest, and Dolder [29], two resonances were found at approximately 19.5 and 26.5 eV. It is hard to imagine how the system could exist with so much energy. In particular, it seems unlikely that any of these resonances are due to the ground-state configuration of O^{--} .

As seen from Figs. 7 and 8, we find no structures that may be related to the existence of doubly charged negative ions (D^{--} and O^{--}). As discussed earlier [30,31], this is for D^- in disagreement with earlier experimental and theoretical results, but is in agreement with recent theoretical considerations [30]. Our result for O^- is also in contrast to the earlier measurement of Peart, Forrest, and Dolder [29], and it appears that the possible influence due to the $1s^2 2s^2 2p^6$ (1S_0)-resonance state at about 6–9 eV is small.

IV. CONCLUSIONS

Electron-impact cross sections for detachment from D^- and O^- have been measured from threshold to 20 and 30 eV, respectively. We found no structure that could be attributed to resonances of the doubly charged negative ions. A charac-

teristic property of the data is the effective threshold at around 2–3 times the binding energy. This is explained by simple classical arguments. Near threshold the collision is adiabatic, and the bound electron will be released only when the perturbing force from the incoming electron exceeds the binding force of the neutral atom. This implies that a substantial fraction of the energy of the incident electron is used to overcome the repulsion from the negative target ion before release can take place. After release, the two continuum electrons carry away kinetic energy due to their Coulomb repulsion. A reaction zone may be defined as the region where the release force exceeds the binding force. The experimental data are in good agreement with a classical reaction model

when a detachment probability of about 10–20 % is assumed. The cross section around the threshold was also with some success described by a model based on tunneling through a barrier, and the low detachment probability in the classical model is ascribed to a tunneling probability which is less than 1 in a large impact-parameter region.

ACKNOWLEDGMENTS

This work has been supported by the Danish National Research Foundation through the Aarhus Center for Advanced Physics (ACAP). Discussions with J. U. Andersen, E. Bonderup, and C. Greene are gratefully acknowledged.

-
- [1] H. S. Massey and E. H. S. Burhop, *Electronic and Ionic Impact Phenomena I* (Oxford University Press, Oxford, 1969).
- [2] *Electron Impact Ionization*, edited by T. D. Mark and G. H. Dunn (Springer, New York, 1985).
- [3] A. Müller, in *Physics of Ion Impact Phenomena*, edited by D. Mathur (Springer, Berlin, 1991), p. 17.
- [4] G. Tisone and L. M. Branscomb, *Phys. Rev. Lett.* **17**, 236 (1966).
- [5] G. Tisone and L. M. Branscomb, *Phys. Rev.* **170**, 169 (1968).
- [6] D. F. Dance, M. F. A. Harrison, and R. D. Rundel, *Proc. R. Soc. London Ser. A* **299**, 525 (1967).
- [7] B. Peart, D. S. Walton, and K. T. Dolder, *J. Phys. B* **3**, 1346 (1970).
- [8] B. Peart, R. Forrest, and K. T. Dolder, *J. Phys. B* **12**, 847 (1979).
- [9] B. Peart, R. Forrest, and K. T. Dolder, *J. Phys. B* **12**, L115 (1979).
- [10] M. R. C. McDowell and J. H. Williamson, *Phys. Lett.* **4**, 159 (1963).
- [11] B. M. Smirnov and M. I. Chibisov, *Zh. Eksp. Teor. Fiz.* **49**, 841 (1965) [*Sov. Phys. JETP* **22**, 585 (1966)].
- [12] M. Inokuti and Y.-K. Kim, *Phys. Rev.* **173**, 154 (1968).
- [13] O. Bely and S. B. Schwartz, *J. Phys. B* **2**, 159 (1969).
- [14] T. L. John and B. Williams, *J. Phys. B* **6**, L381 (1973).
- [15] G. H. Wannier, *Phys. Rev.* **90**, 817 (1953).
- [16] H. Hotop and W. C. Lineberger, *J. Phys. Chem. Ref. Data* **14**, 731 (1985).
- [17] E. P. Wigner, *Phys. Rev.* **73**, 1002 (1948).
- [18] Y. N. Demkov and G. F. Drukarev, *Zh. Eksp. Teor. Fiz.* **47**, 918 (1964) [*Sov. Phys. JETP* **20**, 614 (1965)].
- [19] R. W. Hart, E. P. Gray, and W. H. Guier, *Phys. Rev.* **108**, 1512 (1957).
- [20] E. O. Lawrence, *Phys. Rev.* **28**, 947 (1926).
- [21] B. Peart and K. T. Dolder, *J. Phys. B* **1**, 872 (1968).
- [22] G. H. Dunn, in *Electron Impact Ionization*, edited by T. D. Mark and G. H. Dunn (Springer, New York, 1985), p. 277.
- [23] K. T. La Gattuta and Y. Hahn, *Phys. Rev. A* **24**, 2273 (1981).
- [24] D. S. Walton, B. Peart, and K. Dolder, *J. Phys. B* **3**, L148 (1970).
- [25] D. S. Walton, B. Peart, and K. Dolder, *J. Phys. B* **4**, 1343 (1971).
- [26] B. Peart and K. Dolder, *J. Phys. B* **6**, 1497 (1973).
- [27] H. S. Taylor and L. D. Thomas, *Phys. Rev. Lett.* **28**, 1091 (1971).
- [28] L. D. Thomas, *J. Phys. B* **7**, L97 (1974).
- [29] B. Peart, R. A. Forrest, and K. Dolder, *J. Phys. B* **12**, 2735 (1979).
- [30] F. Robicieux, R. P. Wood, and C. H. Greene, *Phys. Rev. A* **49**, 1866 (1994).
- [31] L. H. Andersen, D. Mathur, H. T. Schmidt, and L. Vejby-Christensen, *Phys. Rev. Lett.* **74**, 892 (1995).
- [32] D. Spence, W. A. Chupka, and C. M. Stevens, *Phys. Rev. A* **26**, 654 (1982).
- [33] L. G. Christophorou, *Adv. Electron. Electron Phys.* **46**, 55 (1978).
- [34] *Recombination of Atomic Ions, Proceedings of the NATO Advanced Research Workshop, Newcastle, Northern Ireland, 1991*, edited by W. G. Graham *et al.*, Vol. 296 of *NATO Advanced Study Institute Series B: Physics* (Plenum, New York, 1992).
- [35] L. H. Andersen, *Comments At. Mol. Phys.* **27**, 25 (1991).
- [36] H. Poth *et al.*, *Z. Phys. A* **332**, 171 (1989).
- [37] L. H. Andersen, J. Bolko, and P. Kvistgaard, *Phys. Rev. A* **41**, 1293 (1990).
- [38] *Electron Cooling and New Cooling Techniques*, edited by R. Calabrese and L. Tecchio (World Scientific, Singapore, 1991).
- [39] A. H. Sørensen and E. Bonderup, *Nucl. Instrum. Methods Phys. Res.* **215**, 27 (1983).
- [40] H. Danared *et al.*, *Phys. Rev. Lett.* **72**, 3775 (1994).
- [41] B. M. Smirnov, *Negative Ions* (McGraw-Hill, New York, 1982).
- [42] G. Fiorentini and R. Tripicciono, *Phys. Rev. A* **27**, 737 (1983).
- [43] V. A. Esaulov, *Ann. Phys. (France)* **11**, 493 (1986).
- [44] D. R. Herrick and F. H. Stillinger, *J. Chem. Phys.* **62**, 4360 (1975).
- [45] J. W. Gadzuk and C. W. Clark, *J. Chem. Phys.* **91**, 3174 (1989).
- [46] S. Huzinaga and A. Hart-Davis, *Phys. Rev. A* **8**, 1734 (1973).